Application of Walnut Shell Biowaste as an Inexpensive Adsorbent for Methylene Blue Dye: Isotherms, Kinetics, Thermodynamics, and Modeling

Sabrina Farch, Madiha Melha Yahoum, Selma Toumi, Hichem Tahraoui, Sonia Lefnaoui, Mohammed Kebir, Meriem Zamouche, Abdeltif Amrane, Jie Zhang, Amina Hadadi, et al.

separations

MDPI

Article

Application of Walnut Shell Biowaste as an Inexpensive Adsorbent for Methylene Blue Dye: Isotherms, Kinetics, Thermodynamics, and Modeling

Sabrina Farch [1,2], Madiha Melha Yahoum [3], Selma Toumi [4], Hichem Tahraoui [4], Sonia Lefnaoui [1], Mohammed Kebir [5], Meriem Zamouche [6], Abdeltif Amrane [7,*], Jie Zhang [8], Amina Hadadi [9] and Lotfi Mouni [9,*]

1 Laboratory of Experimental Biology and Pharmacology, Faculty of Sciences, University Yahia Fares of Medea, Medea 26000, Algeria
2 Laboratory Advanced Materials and Physical Chemistry for Environment and Health, Faculty of Exact Sciences, University Djillali Liabes of Sidi Bel Abbes, Sidi Bel Abbes 22000, Algeria
3 Materials and Environmental Laboratory (LME), University of Medea, Nouveau Pole Urbain, Medea 26000, Algeria
4 Faculty of Sciences, University Yahia Fares of Medea, Medea 26000, Algeria
5 Research Unit on Analysis and Technological Development in Environment (URADTE-CRAPC), BP 384, Bou-Ismail, Tipaza 42000, Algeria
6 Laboratory of Research on Drug Developpement and Sustainable Developpement (ReMeDD), Faculty of Process Engineering, University of Salah BOUBNIDER Constantine 3, Constantine 25000, Algeria
7 University Rennes, Ecole Nationale Supérieure de Chimie de Rennes, CNRS, ISCR–UMR6226, F-35000 Rennes, France
8 School of Engineering, Merz Court, Newcastle University, Newcastle upon Tyne NE1 7RU, UK
9 Laboratory of Management and Valorization of Natural Resources and Quality Assurance, SNVST Faculty, Akli Mohand Oulhadj University, Bouira 10000, Algeria
* Correspondence: abdeltif.amrane@univ-rennes1.fr (A.A.); l.mouni@univ-bouira.dz (L.M.)

check for updates

Citation: Farch, S.; Yahoum, M.M.; Toumi, S.; Tahraoui, H.; Lefnaoui, S.; Kebir, M.; Zamouche, M.; Amrane, A.; Zhang, J.; Hadadi, A.; et al. Application of Walnut Shell Biowaste as an Inexpensive Adsorbent for Methylene Blue Dye: Isotherms, Kinetics, Thermodynamics, and Modeling. *Separations* **2023**, *10*, 60. https://doi.org/10.3390/separations10010060

Academic Editors: Eduardo Díez and Araceli Rodríguez

Received: 1 January 2023
Revised: 11 January 2023
Accepted: 14 January 2023
Published: 16 January 2023

Abstract: This research aimed to assess the adsorption properties of raw walnut shell powder (WNSp) for the elimination of methylene blue (MB) from an aqueous medium. The initial MB concentration (2–50 mg/L), the mass of the biomaterial (0.1–1 g/L), the contact time (10–120 min), the medium's pH (2–12), and the temperature (25–55 °C) were optimized as experimental conditions. A maximum adsorption capacity of 19.99 mg/g was obtained at an MB concentration of 50 mg/L, a medium pH of 6.93 and a temperature of 25 °C, using 0.2 g/L of WNSp. These conditions showed that the MB dye elimination process occurred spontaneously. Different analytical approaches were used to characterize the WNSp biomaterial, including functional groups involved in MB adsorption, the surface characteristics and morphological features of the WNSp before and after MB uptake, and identification of WNSp based on their diffraction pattern. The experimental isotherm data were analyzed by the Langmuir and Freundlich models for the adsorption of MB dye. The corresponding values of parameter R_L of Langmuir were between 0.51 and 0.172, which confirmed the WNSp's favorable MB dye adsorption. The experimental kinetic data were examined, and the pseudo-second-order model was shown to be more suitable for describing the adsorption process, with an excellent determination coefficient (R^2 = 0.999). The exchanged standard enthalpy (H° = −22.456 KJ.mol^{-1}) was calculated using the van 't Hoff equation, and it was proven that the adsorption process was exothermic. The spontaneous nature and feasibility of the MB dye adsorption process on WNSp were validated by negative standard enthalpy values (G°) ranging from −2.580 to −0.469 at different temperatures. It was established that WNSp may be employed as a novel, effective, low-cost adsorbent for the elimination of methylene blue in aqueous solutions.

Keywords: walnut shells; methylene blue; adsorption; analytical approaches; isotherms; kinetic models

1. Introduction

Environmental protection has emerged as a serious priority in our society [1–3]. This has resulted in the development of techniques to enhance methods for cleaning up natural resource pollution, while concentrating on lowering pollution-causing components and protecting public health [4,5]. Water pollution is one of today's most difficult challenges; whether accidental or deliberate, it has resulted in serious environmental issues such as destroying ecosystems, diminishing water quality and endangering human health [6]. It is now attracting considerable interest from a wide range of stakeholders all around the globe (suppliers, academics, lawmakers, organizations, and so on.) [7,8].

Water pollution is caused by the discharge of toxic chemical substances that are not or are only partially biodegradable, such as hydrocarbons, phenolic compounds, heavy metals, dyes, and insecticides, which are commonly found in liquid effluents produced by various industries (chemicals, textiles, tanneries, food, pharmaceuticals, and so on [9,10]. Methylene blue dye (MBD) is a basic organic colorant that is persistent and poorly biodegradable [11], and it is often discharged by industries in excess of the permissible limits set by regulations [12]. The harmful effects of this effluent on local fauna and flora have been reported [13]. To address water pollution, it is critical to develop public and social awareness and enforce severe environmental discharge restrictions. Pollution's potential threats to the ecological balance and human health have been a major worry for public authorities in recent years. Several dye-containing liquid effluent treatments have been employed to reduce their negative effects. Traditional procedures such as nanofiltration [14,15], photodegradation [16], coagulation [17–19], and biological processes provide unsatisfactory results owing to the presence of hazardous chemicals and colors that are difficult to biodegrade in these discharges, due to their complexity that directly influences the efficiency of conventional treatments [20]. Researchers continue to rely on adsorption since it is one of the most extensively utilized techniques that is simple to apply and offers several advantages [21,22]. Adsorption treatment works by trapping dyes with a natural or synthetic material known as an adsorbent. There are various solid materials that may be employed as adsorbents in liquid effluent decolorization procedures, including walnut shells, clay, zeolites, activated alumina, mud, biomass, agricultural residues, and activated carbon [23]. Previous studies have demonstrated that several natural and/or synthetic materials exhibit remarkable adsorption capability for both organic and inorganic compounds and have been thoroughly investigated [24,25]. Because of their low cost, large-scale harvesting, cost-effectiveness, unique properties, abundant fiber, and lignin structures, natural waste materials such as "walnut shells" are regarded viable substitutes for synthetic adsorbents [10,26]. The recovery of natural waste has become an attractive perspective in order to remove cationic and anionic dyes as well as other hazardous chemicals present in aqueous solutions [24,27–29]. Several investigations have shown that owing to their restricted functions, the adsorption capability of certain raw materials is not always sufficient. For example, prior to activation, the biomaterial may have notably poor pore characteristics, limiting its capability to achieve maximum capacity in the adsorption process. According to reports, the performance of these bioadsorbents after suitable physical and chemical treatments also had a significant role in improving their characteristics and providing active and greater surface areas for the elimination of harmful pollutants from industrial wastewater [29,30]. Therefore, according to the scientific literature, the majority of adsorbents need activation prior to use to improve their adsorption capacity. In addition, the absorbent ability of nut shells has been greatly underestimated. According to our knowledge, there has been relatively little interest in using walnut shells to remove colors and other contaminants. This is why our study focused on exploiting the adsorptive properties of raw walnut shells without the need for any prior processing.

In the current investigation, adsorption assays were carried out in order to evaluate the efficiency of the adsorption process of MBD on the WNSp-derived raw powder. The biomaterial was characterized using several analytical methods to assess the influence of various conditions on the MBD adsorption. Several factors were investigated in batch ex-

periments, namely, the initial MBD concentration (2–50 mg/L), the mass of the biomaterial (0.1–1 g/L), the contact time (10–120 min), the medium's pH (2–12), and the temperature (25–55 °C), and modeled to determine their effect upon MBD removal from synthetic dye wastewater. Equilibrium, kinetic and thermodynamic data of MBD adsorption processes onto the adsorbent were also attempted.

Finally, this work is part of the valorisation of waste of natural origin such as raw walnut shells which are biosourced substances, completely renewable and affordable, thus constituting an excellent alternative to synthetic materials and other chemically treated bioadsorbents.

2. Materials and Methods

2.1. Preparation and Characterization of Raw Walnut Shells Powder

The walnut (*Juglans regia*) is a shelled edible fruit. It is produced by walnut trees in the Juglandaceae family. These trees were originally found in temperate environments on the Eurasian and African continents [25]. The procedure of separating the shells from the seeds is easy, straightforward and entirely manual. There were sufficient walnut shells collected to conduct characterization and adsorption testing. The following steps were performed to prepare the raw material: washing, drying, grinding and sieving. In order to prepare the WNSp, initially, the solid residue was washed with tap water until clean washing water was achieved. It was then washed with distilled water to eliminate any remaining dust or particles. The walnut shells were air-dried for 24 h, followed by 48 h in an oven (UN30, Memmert) between 40 and 50 degrees Celsius. The obtained material was crushed and sieved to isolate the fraction with a particle size smaller than 150 m. The chosen fraction was washed many times with deionized water and then dried at 45 °C until a constant mass was reached. The samples were stored until further usage in sealed containers. Before the adsorption experiments, the powder (WNSp) was subjected to a number of tests.

2.2. Adsorbent Characterization

Using the gravimetric technique, the moisture content (% H) of the WNSp was determined. A sample inside porcelain crucibles was placed in an oven (UN30, Memmert) at (1005) °C for 48 h to determine the mass of water evaporated, while drying wet bio-material to a constant mass. The moisture content was determined utilizing the equation [31,32]:

$$\mathrm{H}\,\% \;=\; \left(\frac{\boldsymbol{m_0} - \boldsymbol{m_1}}{\boldsymbol{m_0}}\right)\boldsymbol{x}\;\mathbf{100} \tag{1}$$

where $\boldsymbol{m_0}$ and $\boldsymbol{m_1}$ are the masses of the sample before and after drying (g), respectively.

The zero-charge pH (pHpzc) of adsorbents defines the pH at which the adsorbent surface exhibits clear charge neutrality [33]. The pHpzc of raw WNSp was determined as follows. A set of 0.1 M KNO_3 solutions were prepared in 100 mL closed conical flasks. The initial pH (pHi) of the solutions was adjusted (using 0.1 M of HCl or NaOh) using a pH meter (P-SELECTA pH-2005) to values in the range of 2–12. Subsequently, 0.4 g of raw WNSp was immersed in each solution for 48 h at room temperature with agitation. Filter paper was used to filter the suspension, and the pH of the final filtrate from each mixture was determined. The curve pH = f(pH initial) was drawn (pH = pH final − pH initial). The intersection point of this curve and the abscissa gave the pH at the point of zero charge (pHpzc) of raw walnut shell powder [33,34].

By determining the vibrational properties of chemical functional groups that exist on bio-adsorbent surfaces, Fourier transform infrared spectra was used to reveal functional groups that may be involved in MB adsorption. After the dispersion of anhydrous KBr (1 g KBr per 1 g of material), the WNSp (both before and after MB adsorption) was evaluated using a scanning wavelength range of 400 to 4000 cm^{-1} (FTIR-8400, SHIMADZU). The spectra were captured with a 4 cm^{-1} resolution.

Using a scanning electron microscope (JEOL, JSM 6360) at (25 0.5) °C and an accelerating voltage between 10 kV and 12.5 kV, the microstructure of raw WNSp samples was

studied. At 100 m, the SEM images were captured at magnification levels of ×800. XT microscopy software was used to develop the photomicrographs.

Match 3 software (version 3.12, 2021) was used in combination with a D2 PHASER diffractometer for the XRD analysis (Bruker). Each WNSp sample was analyzed at diffraction angles ranging from 15° to 80° (2).

2.3. Preparation of Dye Aqueous Solution

The cationic reactive dye MBD was provided by Fluka–Analytical. MBD's chemical structure is shown in Figure 1 [35]. It was used without being purified. First, 1 g of dye was dissolved in 1 L of distilled water to make a 1000 mg/L stock solution. This solution was then placed in a black bag and kept in a closet away from light. Then, solutions with various concentrations ranging from 1 to 50 mg/L were generated. By adding either 0.1 M HCl or 0.1 M NaOH, the pH of the solutions was adjusted to the desired level.

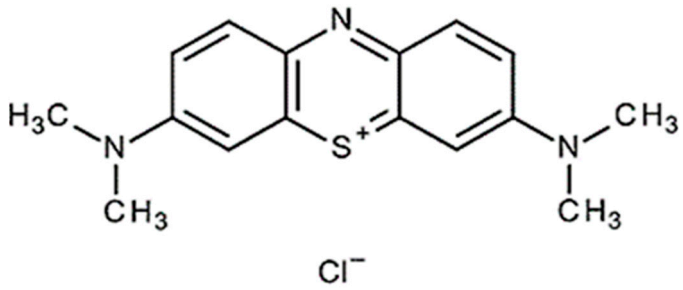

Figure 1. Chemical structure of methylene blue dye.

2.4. Adsorption Experiments

The adsorption tests were conducted by mixing 100 mL of a dye solution with 0.2 g of bio-adsorbent WNSp in Erlenmeyer flasks. Agitation was then performed at 100 rpm until equilibrium was reached. The effect of the main adsorption process parameters, namely pH (2.00 to 12.00), contact time (0.01 to 300 min), initial MBD concentration (1 to 50 mg/L) and temperature (25 to 55 °C), were studied. At the end of the adsorption experiments, the suspension was filtered with 0.40 µm membrane filter paper (What-man filter paper), and the residual concentration of dyes in the liquid phase was determined by measuring their absorbance at a maximum wavelength of 665 nm using a UV-visible spectrophotometer (UV-1600PC). Every experiment was conducted in triplicate, and the mean data are presented. The equilibrium adsorption (q_e, mg/g) and dye removal percentage (R%) were calculated using the following equations:

$$q_e = \frac{(C_o - C_e)}{m} V \quad (2)$$

$$MB\ Removal\ (\%) = \left(\frac{C_o - C_e}{C_o}\right) \times 100 \quad (3)$$

where $\boldsymbol{C_o}$ and $\boldsymbol{C_e}$ (mg/L) are the initial and equilibrium liquid concentrations of the dye solutions, respectively, $\boldsymbol{V}$ is the volume of the MBD solution (L) and $\boldsymbol{m}$ is the mass of the prepared adsorbent (g).

3. Results and Discussion

3.1. Biosorbent Characterization

3.1.1. FTIR Analysis

Using FTIR analysis, the functional groups of the bio-adsorbent surface and their alterations throughout the adsorption process were determined. The spectra of WNSp before and after MBD adsorption are shown in Figure 2. The observed absorption bands demonstrate and validate the existence of WNSp-specific bindings. The largest peaks of raw WNSp occurred in the functional group region at 3419 cm^{-1}, 2926 cm^{-1}, and 1614 cm^{-1}

(Figure 2a). The broad peak that occurred at 3419.35 cm^{-1} is attributed to the stretching vibration of the hydroxyl functional group (-O-H), and that of 2926.84 cm^{-1} is due to the C–H stretching vibration of alkane [36,37]. The band at 1746.13 cm^{-1} is attributed to C=O stretching of the carbonyl group, and the band observed at 1614.57 cm^{-1} may be attributed to the alkene C=C stretching of the aromatic ring present in lingnine. These results showed the presence of cellulose, hemicelluloses and lignin, as major constituents of walnut shells structure [36].

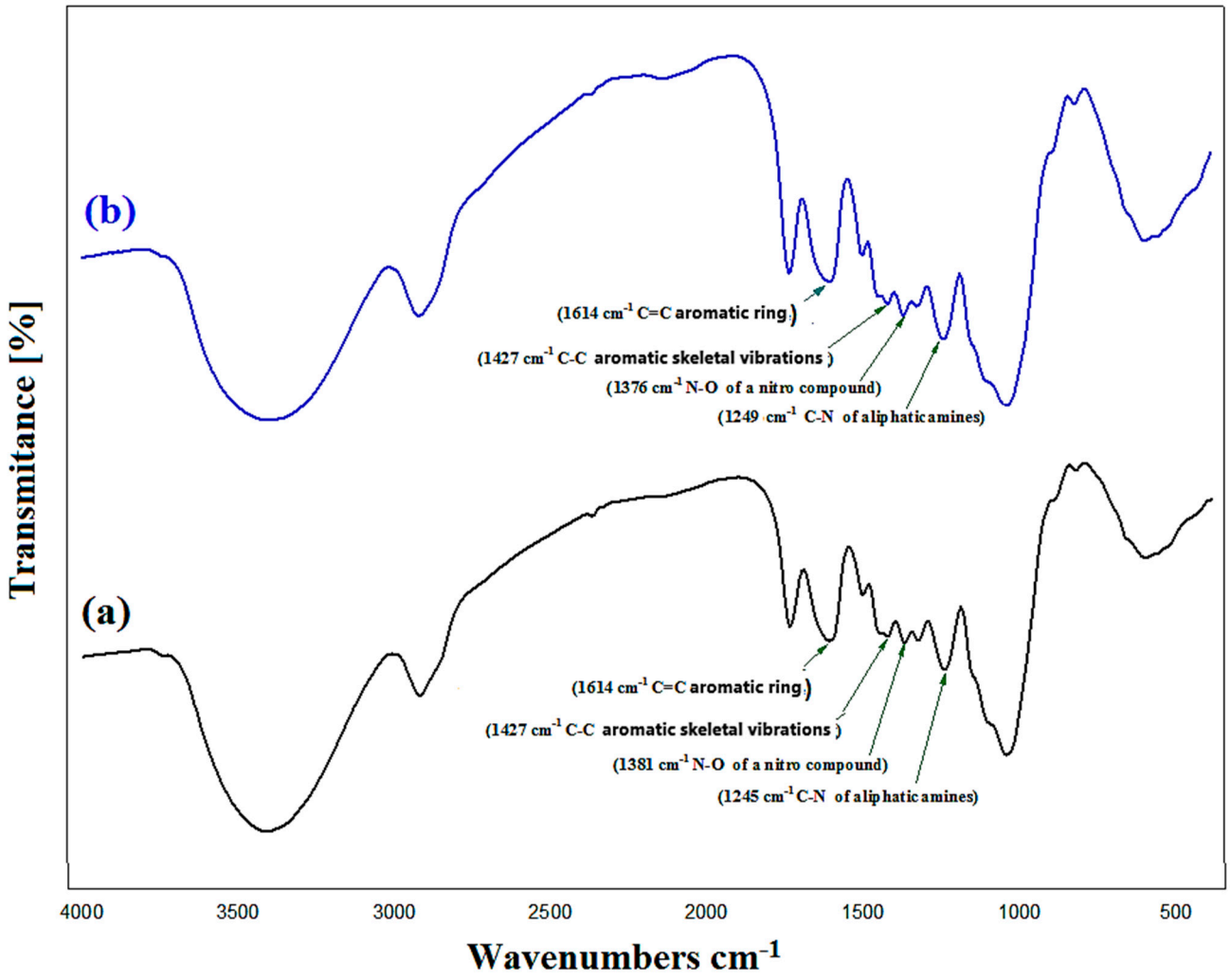

Figure 2. FTIR spectra of raw walnut shells powder: (**a**) before and (**b**) after MBD adsorption.

Figure 2b clearly demonstrates a change in the location of several functional groups regarded as possible adsorption sites, such as hydroxyl, carbonyl, and carboxyl, after the adsorption of MBD. These distinct changes confirm the active involvement of the given functional groups. Thus, the prominent peaks associated with raw WNSp, as detected at 1432.04 cm^{-1}, 1381.06 cm^{-1}, 1245.4 cm^{-1}, and 1045.6 cm^{-1}, might be attributed to the presence of a variety of aromatic, aliphatic, and nitro substances [38,39]. The peaks might be attributed to aromatic ring C-C stretching, nitro compound N-O stretching, or aliphatic/aromatic amine C-N stretching [40]. Following adsorption, these peaks are relocated to different positions of 1427.93 cm^{-1}, 1376.95 cm^{-1}, 1249.51 cm^{-1}, and 1049.71 cm^{-1}, which denotes the involvement of the aforementioned groups [41,42].

Furthermore, the dye-loaded WNSp spectrum exhibits a slight change in the transmittance of the strong peak at 1614.57 cm^{-1} and an increase in the intensity of the peak at 2926.84 cm^{-1} attributed to the C–H stretching vibration of alkane, probably due to the

presence of the methyl groups in the MBD molecule [36]. This peak corresponds to the amine functional group's vibrational band, which is involved in H-bond formation [36]. The sharp and narrow peak at 1045 cm^{-1} is assigned to the carbohydrate content in WNSp. This peak demonstrated a shift to 1049 cm^{-1} after MBD adsorption onto WNSp [40]. After MBD adsorption by raw WNSp, the FTIR spectrum shows significant changes that confirm WNSp's efficiency as a natural MB adsorbent. In addition, the preceding data show that the adsorption mechanism involves methylene blue with functional groups present in the biomass.

3.1.2. Scanning Electron Microscopy Analysis (SEM)

A scanning electron microscope (SEM) was used to examine the surface characteristics and morphological features of the WNSp before and after MBD adsorption kinetics. The surface morphology of raw walnut shell powder prior to and after adsorption is shown in Figure 3. According to (Figure 3a) before adsorption, the WNSp has an amorphous nature, heterogeneous morphology and substantial porosity and hardness. In the second picture (Figure 3b), the SEM reveals the less porous surface of the raw WNSp and a more uniform morphology owing to the stacking of MBD in the structure's porosity and the formation of a thick layer on the surface of the structure after MBD adsorption. The obtained findings demonstrate the adsorption efficiency of MBD onto raw WNSp.

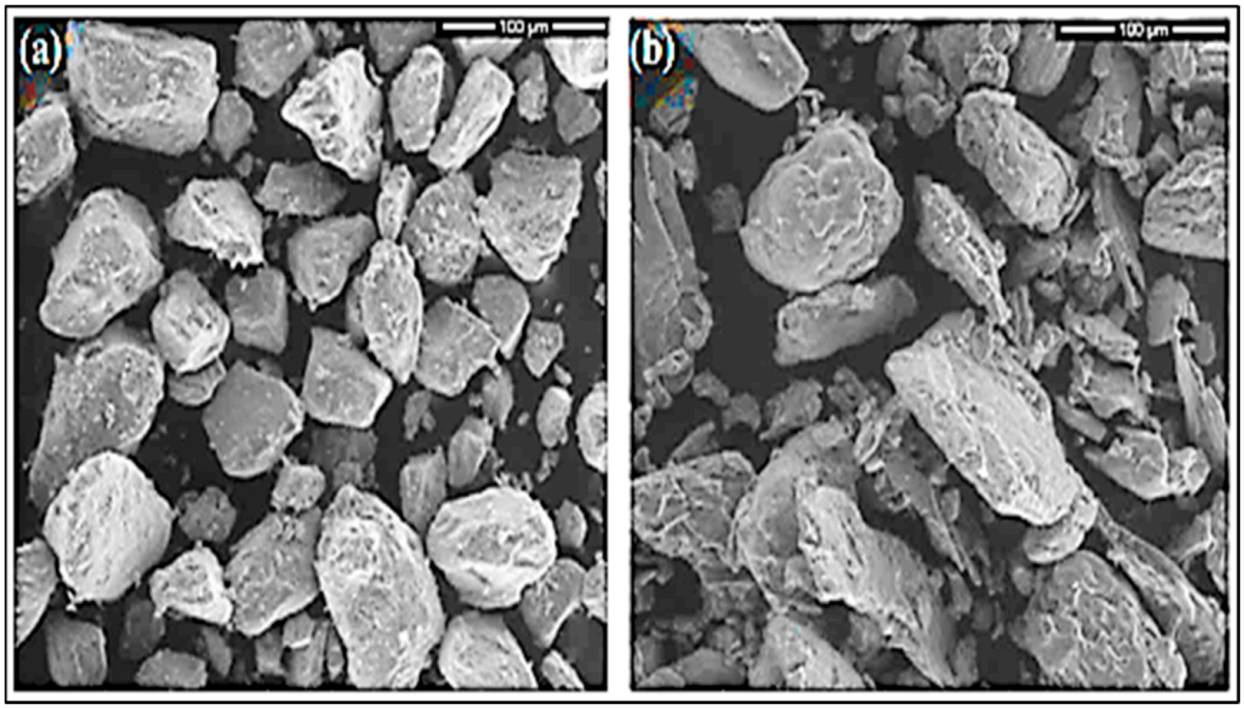

Figure 3. SEM image of raw WNSp (**a**) before and (**b**) after MBD adsorption (100 µm, 800×, 10 kV).

3.1.3. X-ray Diffraction (XRD)

The raw WNSp XRD spectrum suggests that the powder is amorphous (Figure 4). Indeed, the amorphous section in Figure 4a, shows a large peak in the 2θ range of 17–24°, which is typical of cellulose I, as well as fine peaks between 33 and 34°. An increase in cellulose content can explain the high intensity of the WNSp spectra [26]. After adsorption of MBD, the XRD spectrum showed a reduction in the intensity of the peak located around 2θ = 33–34° and the appearance of a short peak of low intensity at 2θ around 45–46° (Figure 4b). The XRD results indicate that WNSp has conserved its amorphous nature despite the presence of MBD in the biomaterial structure [43]. Therefore, the XRD analysis showed that the adsorption of MBD did not affect the structure of the WNSp.

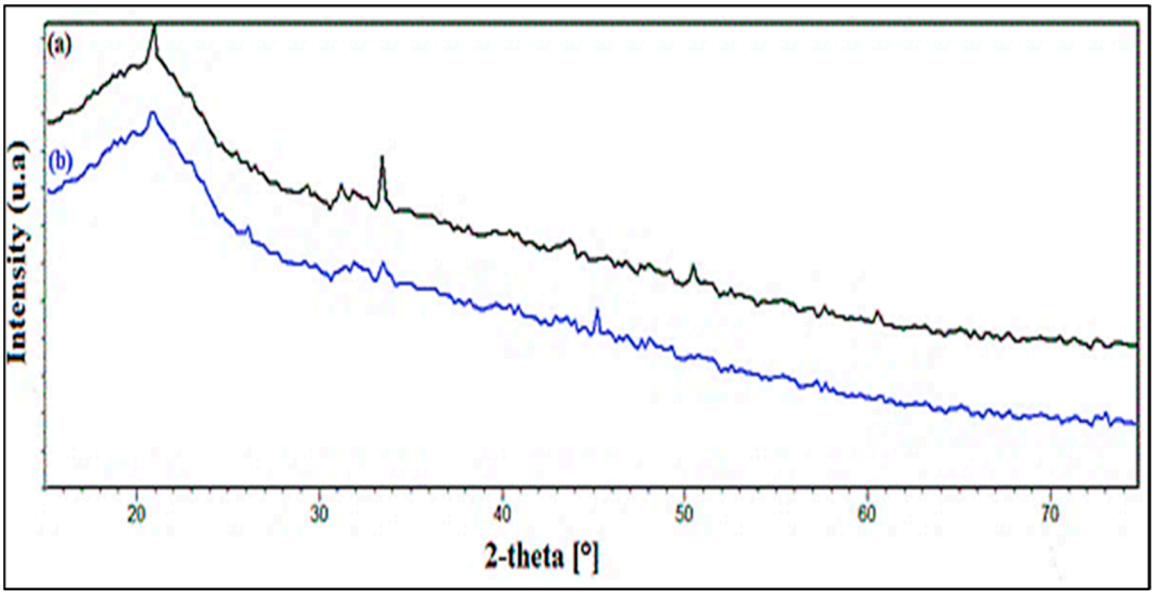

Figure 4. XRD spectra of raw WNSp (**a**) before and (**b**) after MBD adsorption.

3.2. The Influence of Different Factors on MBD Adsorption onto Walnut Shells

3.2.1. Effect of Initial pH on Adsorption

The pH point of zero charge (pHpzc) is a crucial parameter in adsorption phenomena that defines the electrostatic interaction of the adsorbate and adsorbent and is described as the pH level at which the adsorbent's surface charge equals zero [44,45]. The results for the determination of pHpzc are shown in Figure 5a. The pHpzc value was 6.93. At pH values greater than the pHpzc (pH > 6.93), due to the cationic dye ions' propensity to be attracted to the solid surface, the electrostatic interaction between the negative adsorbent and cationic dye (MBD) increased, increasing adsorption efficiency [46]. On the other hand, the decrease in removal efficiency at low pH values (pH < 6.93) was due to the positively charged surface of WNSp that repelled the cationic dye molecules.

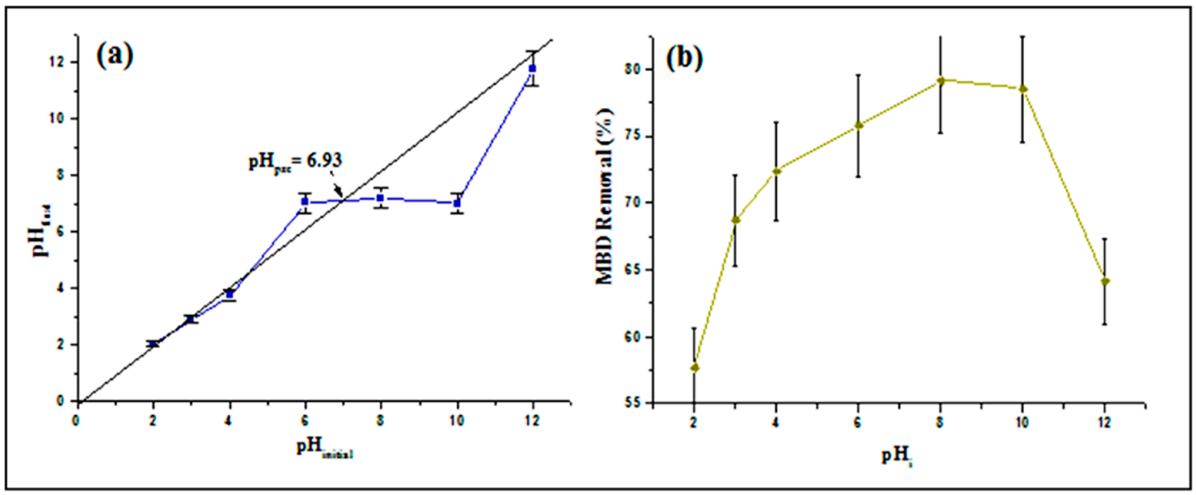

Figure 5. (**a**) pH at point of zero charge (pH_{pzc}), and (**b**) effect of pH on MBD adsorption.

The initial pH value of the solution is one of the critical factors in the adsorption process that can influence the adsorptive capacity of the adsorbent [47]. The effect of initial pH on MBD adsorption was investigated at initial pH values ranging from 2 to 12, and the findings are shown in Figure 5b. The experiments were performed with a specific dye concentration of 50 mg.L^{-1} (V= 100 mL), a temperature of 25 °C, a stirring speed of

300 rpm and an adsorbent mass of 0.2 g. According to the findings, the adsorption yield increased slightly with increasing pH, reaching a maximum of 79.14% at pH = 8. At low pH levels (2.4 and 6), H^+ ions would surround the surface of the adsorbent, decreasing the interaction between methylene blue ions and raw WNSp sites. However, at higher pH values, the anionic groups present on the WNSp'surface are ionized, thus promoting electrostatic attraction with the cationic MBD molecule until pH 8 is reached. At this pH, the greatest adsorption capacity is obtained due to maximum electrostatic equilibrium. Beyond this pH, the adsorption capacity begins to decline due to the fact that in a strong alkaline environment, the anionic charge density is very high, whereas the positive charge of the MBD was almost neutralized which results in lower electrostatic interactions.

3.2.2. Effect of the Adsorbent Mass on MBD Adsorption onto Walnut Shells

The adsorbent mass has a substantial influence on the efficiency of raw WNSp in removing methylene blue dye from aqueous solutions. To investigate the influence of adsorbent mass in the sorption experiments, tests were conducted using 0.2 g to 1 g of raw WNSp adsorbent to assess the influence adsorbent's mass. Figure 6 displays the impact of the adsorbent mass on the adsorption process. The amount of removed MBD increased with the increase in adsorbent mass, reaching the highest removal rate of (81.42%) using 1 g of raw WNSp. This may be attributed to the increasing number of pores on the adsorbent surface, thus providing more adsorption sites. The adsorption capacities of MBD onto raw WNSp were 486.70 mg/g, 97.20 mg/g, 63.3 mg/g, 50.12 mg/g, and 40.71 mg/g at 0.2, 0.4, 0.6, 0.8, and 1 g/L adsorbent masses, respectively. According to the data, the quantity of adsorbed dye per unit mass (mg/g) decreases as the amount of adsorbent increases [32,48].

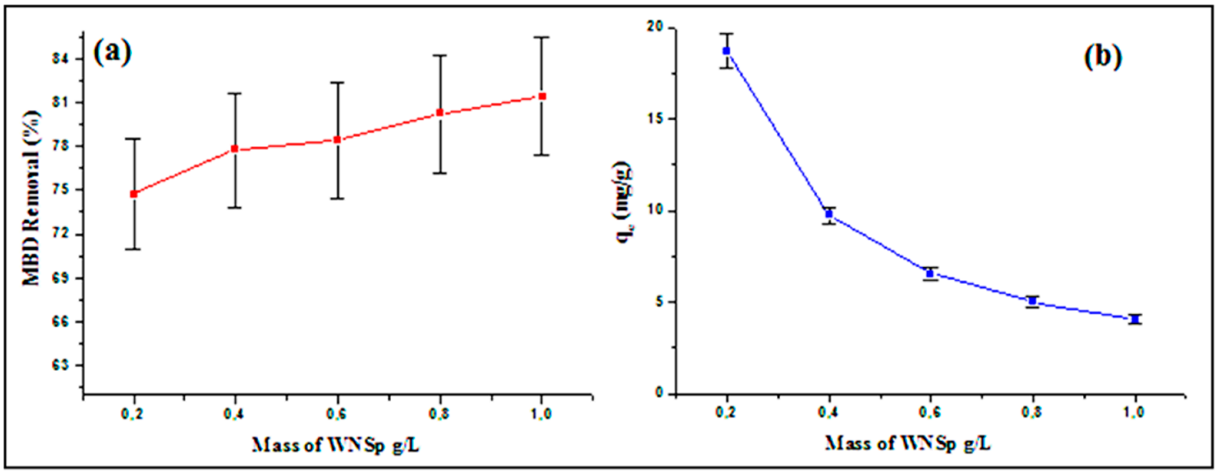

Figure 6. (**a**) Effect of adsorbent mass on MBD removal (**b**) Influence of the adsorbent mass on the adsorption capacity of the MBD.

3.2.3. Effect of the Initial Dye Concentration

The effect of the initial MBD concentration on the percentage of elimination was examined by varying the initial MBD concentration from 10 to 50 mg/L, while all other parameters were maintained constant. As shown in Figure 7, the equilibrium adsorption capacity increased from 0.03 mg/g to 19.995 mg/g with increasing MBD concentration (10 to 50 mg/L). The greater potential was created by higher MBD concentrations, and therefore, higher adsorption yields were attained [49,50]. A general trend of increasing rate of MBD adsorption with increasing initial MBD concentration was observed (Figure 7a). The results show that the rate of adsorption increases proportionally with the initial concentration of MBD less than 30 mg/L. Further than that, the adsorption rate gradually increased at initial values between 30 and 50 mg/L. This means that at high dye concentrations, the ratio of adsorption active sites to total dye molecules in solution is low, thus slowing down the interaction of the dye molecules with the WNSp. Figure 7b shows a

plot of the amount of dye adsorbed (q_e) versus initial dye concentration. For an increase in initial dye concentration from 10 to 50 mg/L, the amount of dye adsorbed increases from 0.03 to 19.995 mg/g, as shown in the graph. As a result, all MBD molecules in the medium could potentially interact with the adsorbent's surface binding sites.

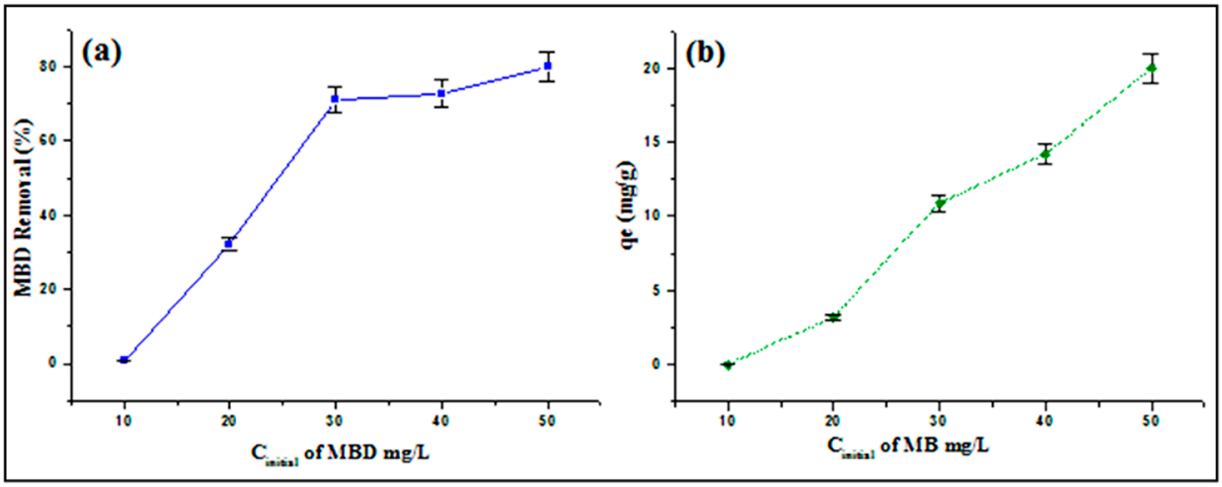

Figure 7. (**a**) Effect of the initial MBD concentration on MBD removal and (**b**) on the adsorption capacity of raw WNSp.

3.2.4. Effect of the Contact Time

The contact time corresponding to the adsorption/desorption equilibrium is determined as part of the kinetic analysis of the MBD adsorption on the WNSp in solution. Regardless of other experimental parameters affecting the adsorption kinetics, the contact time has a considerable influence. Adsorption studies were carried out to determine the influence of contact time on MBD adsorption onto the WNSp surface in a MBD solution with an initial concentration of 50 mg/L. At room temperature, at an agitation rate of 100 rpm, the time interval observed ranged from 0 to 300 min. Adsorption isotherms for raw WNSp were established after determining the contact time and adsorption equilibrium. This is critical for evaluating whether monolayer or multilayer adsorption is achievable and estimating the maximum adsorption capacity. Adsorption efficiency as a function of time was plotted to determine the contact time between WNSp and the MBD solution (Figure 8). The findings revealed that the quantity of MBD adsorbed increased fast in the first 30 min (part 1), when the conditions for adsorption were optimal. A rate of 84.92% showed a gradual and slow equilibrium between 30 and 75 min, suggesting a pre-equilibrium condition (intermediate part). This demonstrates that the bioadsorbent's adsorption of the dye was quite fast. The adsorption then steadily decreased.

This was because there were a lot of active sites on the surface of raw WNSp during the early phases of adsorption [51,52]. However, occupying the remaining empty sites proved difficult in the later phases. This resulted from the development of repulsive interactions between the MBD molecules on the solid's surface and those in the aqueous phase. Furthermore, the MBD molecules were medium in size and could readily diffuse through the internal pores until they were saturated, ultimately leading to a reduction in the mass transfer between the liquid and solid phases over time. The rate of adsorption was decreased from 75 to 120 min, and a plateau was observed that corresponded to the condition of equilibrium after 120 min (part 2). Based on these findings, the equilibrium duration in kinetic adsorption studies was set at 120 min (85.54%) [52]. F. Lansari et al. [50] conducted one of numerous investigations that emphasized these findings.

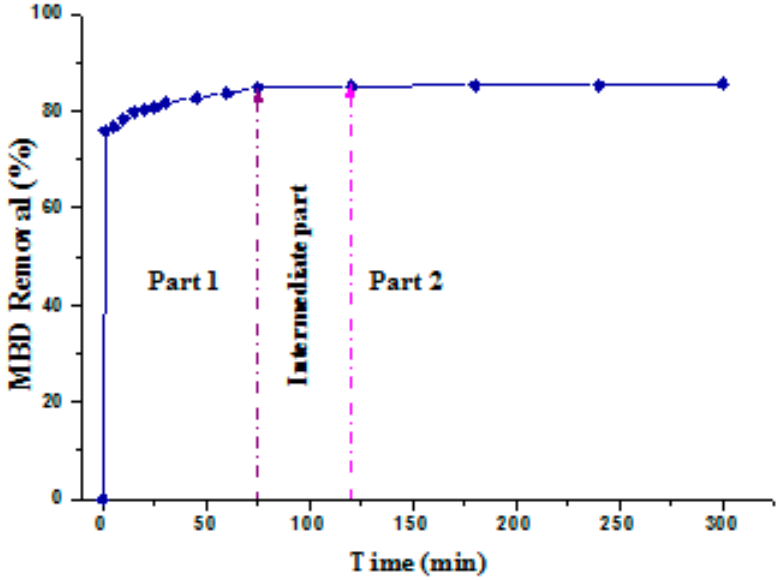

Figure 8. Effect of the contact time on the adsorption of MBD with raw WNSp.

3.2.5. Effect of Temperature

One of the main parameters that might impact the adsorption process is temperature. The adsorption of MBD from an aqueous solution was investigated at temperatures ranging from 25 to 35 to 55 °C. The findings of this investigation revealed that increasing the temperature reduced adsorption effectiveness. However, since the system quickly reached equilibrium, the increase in temperature enhanced the adsorption rate. Adsorption effectiveness decreases with increasing temperature, implying that adsorbent surface activity decreases as temperature increases. The physical bond between the dye molecules and the active sites of the adsorbent weakens, and MBD adsorption is governed by physical forces [53]. Figure 9 depicts the obtained results. The adsorption capacity increased to a maximum of 21.25 mg/g at a temperature of 25 °C. Beyond this temperature, the removal effectiveness of MBD decreased gradually from 85 to 70.38% as the temperature increased from 25 to 55 °C, indicating that MBD adsorption on raw WNSp was exothermic and that a low temperature favored adsorption. As a consequence, the best results were achieved in the ambient temperature range [54].

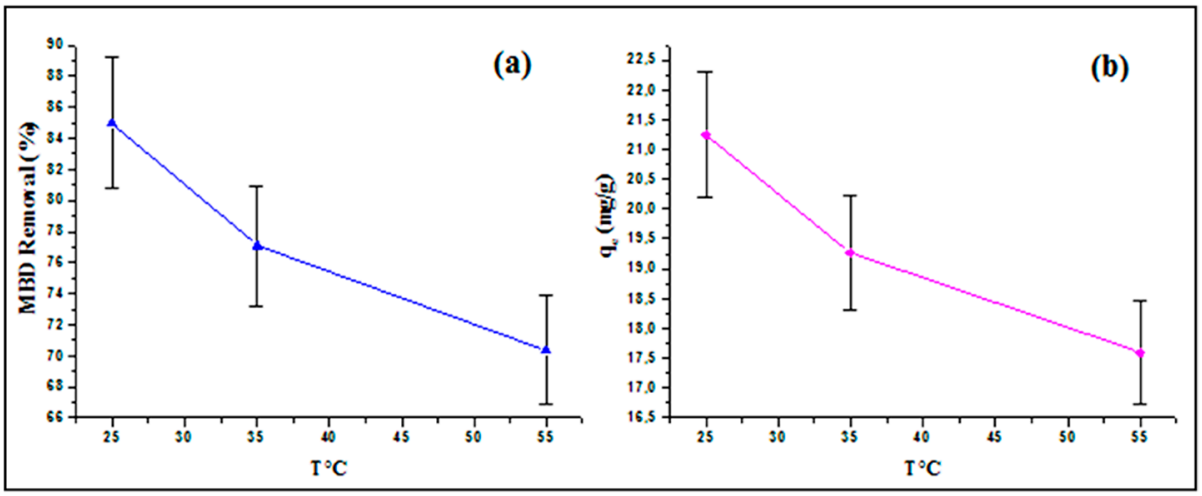

Figure 9. (**a**) Effect of temperature on MBD removal and (**b**) on the adsorption capacity of MBD with raw WNSp.

3.2.6. Adsorption Equilibrium Study of MBD by Raw WNSp Adsorbent

In general, understanding adsorption isotherms is crucial for selecting an appropriate correlation of equilibrium information and optimizing the design of an adsorption system [45]. Two isotherm equations, notably the Langmuir and Freundlich isotherms, were used in this investigation [55,56] to assess the balance of MBD at different initial concentrations ranging from 10 to 50 mg/L under stirring at 100 rpm for 300 min of adsorption by introducing 0.2 mg of raw WNSp, pH 6.93 and at room temperature. When the suspension reached equilibrium, it was filtered and the MBD solution was measured. The adsorption isotherms were derived by plotting $q_e = f(C_e)$, where q_e and C_e are the quantity of adsorbed dye per gram of adsorbent and the concentration at the dye equilibrium, respectively (Figure 10). This study primarily focused on the Langmuir and Freundlich adsorption isotherms to allow the determination of the mechanism of MBD adsorption on raw WNSp, the maximum quantities of dye adsorbed, and the affinity of the adsorbate towards the adsorbent.

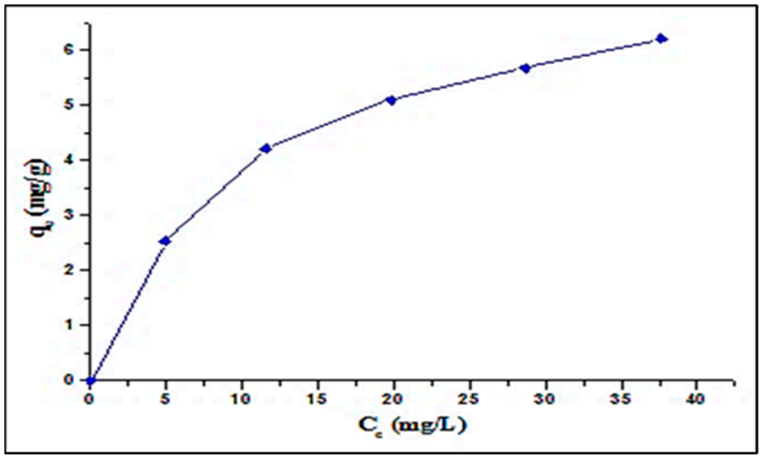

Figure 10. Isotherm of adsorption of MBD on raw walnut shells powder.

The initial concentration of MB dye steadily increased the adsorption capacity but it did not reach maximal saturation. It is, more specifically, an L-type isotherm, as described by Giles et al. [57]. This form of isotherm often occurs when the solute molecules adsorb flat on the surface and there is no competition for adsorption sites between the molecules of the solvent and dye [58].

The obtained results are comparable with those of other works reported in the literature for various agricultural raw or activated adsorbents, as summarized in Table 1.

Table 1. Comparison of adsorption capacity of MBD onto raw WNSp various adsorbents.

Dye	Adsorbent	MB Dye Removal (%)	Reference
Methylene blue	Walnut shell bio-waste	80 %	This work
Methylene blue	levulinic acid-modified natural shells	98.13%	[59]
Methylene blue	Carboxymethyl cellulose/carboxylated graphene oxide composite microbeads	97.97%	[60]
Methylene blue	Mesoporous activated carbon with high surface area from KOH-activated dragon fruit peels	92.3%	[61]
Methylene blue	Acid-factionalized biomass material	83 %	[62]
Methylene blue	Agricultural Products	93.2 %	[63]
Methylene blue	Waste of orange and lemon peels derived activated carbon	96 %	[64]

3.2.7. Modeling of Adsorption Isotherms

The goal of this section is to precisely characterize the experimental data of the MBD's adsorption isotherms by the WNSp utilizing the Langmuir and Freundlich models.

Langmuir Model

The Langmuir adsorption isotherm is the most widely used model for describing the equilibrium between adsorbate and adsorbent material in monolayer and homogeneous sorption and also without interaction among the adsorbed molecules. According to this interpretation, once the MBD molecule occupies an adsorbent site, no additional adsorption may occur at that location [58]. The following equation [65,66] depicts the linear version of the Langmuir isotherm model:

$$\frac{C_e}{q_e} = \frac{C_e}{q_m} + \frac{1}{K_L q_m} \quad (4)$$

where C_e (mg/L) represents the equilibrium concentration of the MBD in the solution, q_e (mg/g) is the adsorption capacity of raw WNSp at equilibrium, q_m (mg/g) is the maximum adsorption capacity of MBD solute fixed per unit mass of raw WNSp and K_L (L/mg) is the effective dissociation constant that relates to the affinity binding position; these constants are related to the adsorption energy and adsorption capacity.

Following the modeling of experimental results, the values of Langmuir constants q_m and K_L are obtained from the intersection and the slope of the linear plot of C_e/q_e against C_e (Figure 11a) and are presented in Table 1.

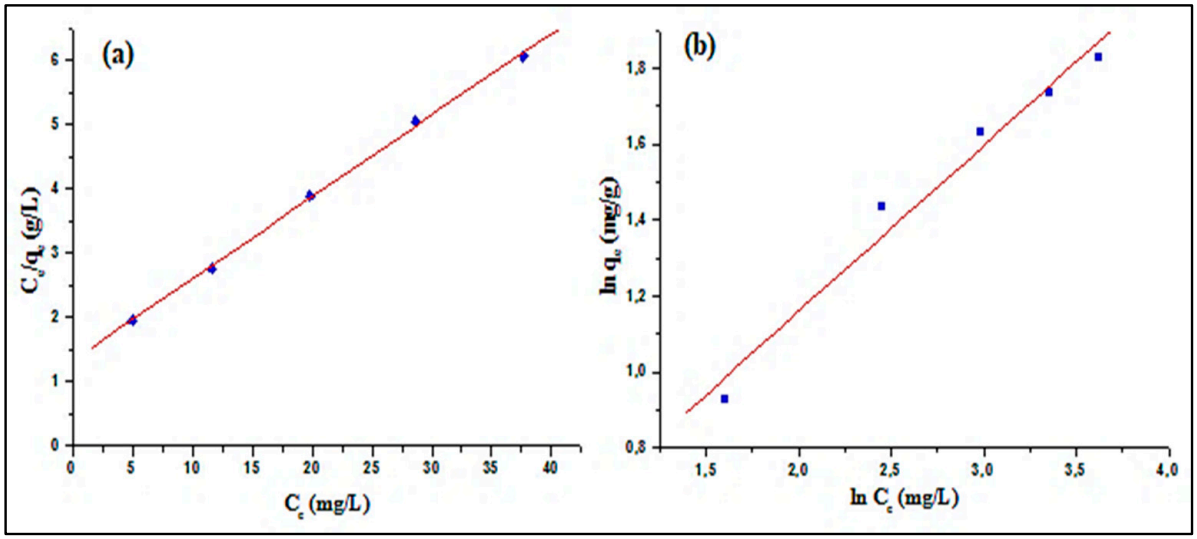

Figure 11. (**a**) Langmuir isotherm model for the adsorption of MBD on raw WNSp. (**b**) Freundlich isotherm model for the adsorption of MBD on raw WNSp.

The essential properties of the Langmuir isotherm may be stated in terms of a dimensionless parameter RL, also known as the equilibrium parameter, and determined by the following equation [67]:

$$R_L = \frac{1}{(1 + K_L * C_o)} \quad (5)$$

where C_o is the initial MBD concentration (mg/L); the estimate of R_L suggests the Langmuir isotherm that is favorable for adsorption ($0 < R_L < 1$), results in irreversible adsorption ($R_L = 0$), linear ($R_L = 1$) or is unfavorable for adsorption ($R_L > 1$) [68].

The plot of the Langmuir equation showed a good correlation ($R^2 = 0.9996$). These findings validate the hypothesis that adsorption occurs at sites that are sufficiently separated from one another for the adsorption to behave according to the Langmuir adsorption

site independence model. It is concluded that the adsorption of the MBD by the WNSp follows the Langmuir model. This implies that the adsorption sites on the solid's surface are all energetically equivalent and that each site can fix only one molecule. Furthermore, adsorption occurs in monolayers, and no intermolecular interaction was detected. Finally, the corresponding RL values varied between 0.5099 and 0.1722, confirming that the MBD was effectively absorbed by raw WNSp. This demonstrated that the elimination of MBD was a spontaneous process.

Freundlich Model

The Freundlich isotherm model, in contrast to the Langmuir isotherm, describes the heterogeneous adsorption of MBD molecules at different positions with different space energies of adsorption. As a result, the amount of MBD adsorption on the WNSp varies with the exponential distribution of locations and adsorption energies. The following equation (Equation (6)) was used to obtain the linear form of the Freundlich isotherm [69]:

$$\text{Ln } q_e = \ln k_F + \frac{1}{n} \ln C_e \quad (6)$$

where k_F and n represent the Freundlich adsorption isotherm constants, which indicate adsorption intensities and adsorption capacity of the adsorbent, respectively. C_e is the equilibrium concentration of solution MBD in the equilibrium solution (mg/L), and q_e is the amount of MBD adsorbed per unit weight of raw WNSp (mg/g).

The Freundlich isotherm equilibrium constants KF and 1/n are associated with sorption capacity and sorption intensity of the system and can be plotted as a function of ln q_e versus ln C_e, which is represented by the linear relationship presented in Figure 11b with the values given in Table 2. When the number is $1/n > 1$, both adsorption intensity and isotherm type are required, and the adsorption capacity increases as new adsorption sites arise. Nevertheless, when $1/n > 1$, the adsorption bond is weakened, which leads to difficult adsorption, contributing to a decline in the adsorption capacity [65].

Table 2. Langmuir and Freundlich isotherm constants for MB dye adsorption.

Langmuir Y= 1.3245 + 0.1274 X			**Freundlich** Y= 0.2862 + 0.4369 X		
q_{max} **(mg.g^{-1})**	K_L **(L.mg^{-1})**	**R²**	***n***	K_F **(mg$^{1-1/n}$·L$^{1/n}$·g^{-1})**	**R²**
7.849	0.096	0.999	2.288	1.331	0.986
SD	***p***		***SD***	***p***	
0.0626	<0.0001		0.6649	0.0018	

The Langmuir and Freundlich isotherms were employed to analyze the MBD removal experimental results (Figure 11). The determination coefficient (R^2) was established to evaluate the isothermal models. Thus, the Langmuir isotherm fits the constant equilibrium of MBD removal by raw WNSp with a determination coefficient of $R^2 = 0.9994$, confirming monolayer physical type adsorption.

3.2.8. Adsorption Kinetic Models

Experimental kinetic data were examined using a pseudo-first-order model [70] and pseudo-second-order model [71] to investigate the adsorption kinetics of MBD. Each model proposes hypotheses about the most likely mechanisms; these two models are represented as follows:

❖ **Pseudo-First-Order Model**

The Lagergren model is an irreversible kinetic model based on the amount of dye adsorbed on the surface of the particle. It can be represented by the following equation:

$$ln\ (q_e - q_t\ )\ =\ ln\ q_e - K_1.t \quad (7)$$

where q_e is the amount of MB dye adsorbed per unit mass of the adsorbent raw WNSp at equilibrium (mg/g), q_t is the quantity of MBD adsorbed per unit mass of the adsorbent WNSp at time t (mg/g), t is the contact time in minutes, and K_1 is the speed constant of the pseudo-first-order adsorption (1/min) [72,73], The validity of this model can be verified by the linearization of ln ($q_e - q_t$) as a function of time.

❖ **Pseudo-Second-Order Model:**

Ho and McKay's model assumes heterogeneity of the fixation sites, constant adsorption energy independent of the overlap rate of the sites, and no interaction between the adsorbed molecules. It also suggests a chemisorption mechanism. Adsorption equilibrium capacity determines the latter, which is represented by:

$$\frac{t}{q_t} = \frac{1}{q_e^2.K_2} + \frac{t}{q_e} \quad (8)$$

where K_2 is the second-order rate constant (g/mg.min) that can be defined experimentally from the slope and interception of the t/q_t line as a function of time [74].

Table 3 summarizes the results of the kinetic model representation (Figure 12) that were used to analyze the adsorption kinetic constants of WNSp at 0.2 g/L. The results show that the pseudo-second-order model was more suitable for defining the adsorption process, with an excellent coefficient of determination (R^2 = 0.9998) and a quantity of MBD adsorbed per unit of raw WNSp mass at the equilibrium q_e value of 2.2888 mg/g. This indicated that chemical adsorption contributed to the fixation of the MBD on the raw WNSp [75]. Similar results were previously reported on the removal of MBD using many other biomass adsorbents, such as rice hull ash, *Citrus limetta* peel, wheat straw, and shaddock peel, where a pseudo second-order model described the adsorption kinetics [43].

Table 3. Kinetic models for the adsorption of MBD onto raw WNSp.

Pseudo-first order Y= 0.9691 + (−0.0357) X			***Pseudo-second order*** Y= 0.0406 + 0.0470 X		
q_e **(mg/g)**	K_1 **(1/min)**	R^2	q_e **(mg/g)**	K_2 **(g/mg·min)**	R^2
2.635	0.0357	0.969	2.288	0.074	0.999
SD		***p***	***SD***		***p***
0.2345		<0.0001	0.023		<0.0001

3.2.9. Thermodynamic Adsorption and the Effect of Temperature

Since the adsorption capacity is significantly influenced by temperature, assessing the adsorption temperature is considered a primary step to distinguish between chemisorption and physisorption. As represented in Figure 9, the adsorption removal efficiency decreased as temperature increased. MBD had a maximum adsorption capacity of 21.25 mg/g at 25 °C. Increasing the solution temperature from 25 °C to 55 °C decreased the dye removal efficiency. This indicates that the biosorption process was exothermic.

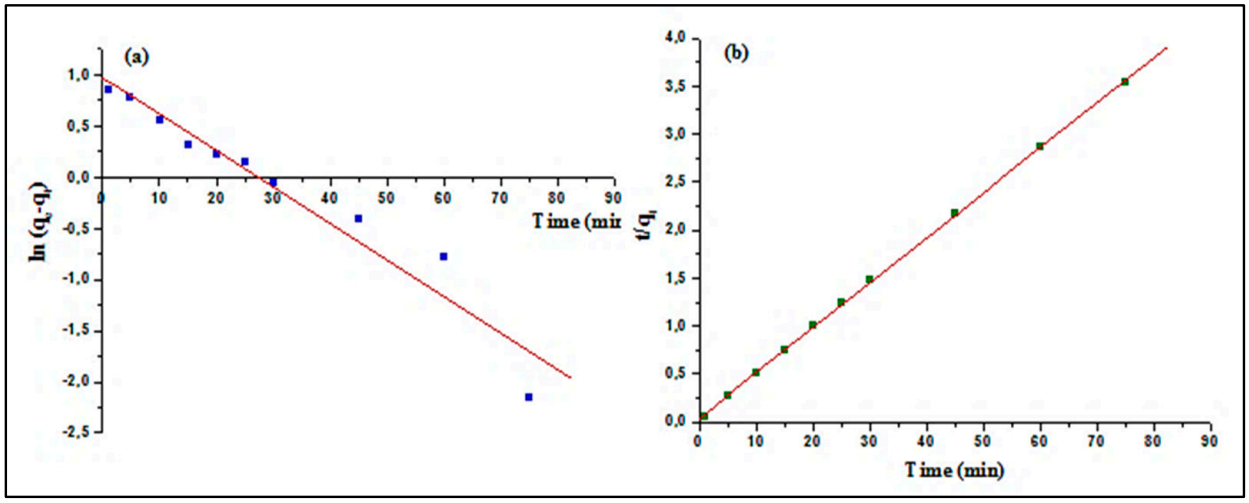

Figure 12. Kinetics of MBD adsorption by raw WNSp: (**a**) pseudo-first-order kinetics, and (**b**) pseudo-second-order kinetics.

The state of equilibrium in the chemical and physical reactions in the adsorption process is related to thermodynamics. The changes in the enthalpy (ΔH^0), entropy (ΔS^0), and Gibbs energy (ΔG^0) of an adsorption process are identified by thermodynamic parameters. The thermodynamic characteristics may be used to assess whether the adsorption phenomena was endothermic or exothermic [76]. The values of enthalpy (ΔH^0), entropy (ΔS^0), and Gibbs free energy (ΔG^0) are determined from the intercept and slope of the Van't Hoff plot. The thermodynamic parameters were calculated using the formulae shown below [66]:

$$\mathbf{\Delta G^0 = -RT \ln K_e} \quad (9)$$

$$\mathbf{\ln K_e} = -\frac{\Delta H^0}{RT} + \frac{\Delta S^0}{R} \quad (10)$$

$$\mathbf{\Delta G^0} = \mathbf{\Delta H^0 - T\,\Delta S^0} \quad (11)$$

where R is the ideal gas constant (8.314 J/mol K), K_e is the equilibrium constant of the adsorption process expressed in qe/Ce and T is the absolute temperature in Kelvin (K). The enthalpy (ΔH^0) and the entropy (ΔS^0) were determined from the slope of the regression line obtained by carrying ln K_e as a function of 1/T, and then the parameter ΔG^0 was determined from the above equation for different temperatures.

The calculated values of the parameters ΔG^0, ΔS^0, and ΔH^0 are presented in Table 4.

Table 4. Thermodynamic parameters of MBD adsorption onto raw WNSp.

ΔH° (kJ/mol)	ΔS° (kJ/mol·K)	ΔG° (kJ/mol) Y= −8.1118 + 2701.0968 X			R^2	SD	*p*
		T = 298 K	T = 308 K	T = 328 K			
−22.4569	−0.0674	−2.580	−1.330	−0.470	0.9607	0.1717	0.1790

The van 't Hoff equation was used to calculate the exchanged standard enthalpy ($\Delta H^\circ = -22.457$ KJ.mol^{-1}), which indicated an exothermic adsorption process [76]. The negative standard enthalpy values (ΔG°), which varied from −2.580 KJ.mol^{-1} to −0.470 KJ.mol^{-1}, confirmed the spontaneous nature of the adsorption process of the MBD on raw WNSp [59,77]. The decrease in ΔG° values with increased temperature indicates the highly efficient adsorption at low-temperature values [78,79]. Furthermore, the negative value of ΔS° suggests a decrease in disorder at the solid–solution interface. Similar studies have reported that the negative value of entropy indicates that MBD molecules were less organized in the

solution, and were deposited on the raw WNSp surface without any significant changes to the internal structure of raw WNSp along the adsorption process [43].

4. Conclusions

The adsorption of methylene blue dye by raw WNSp was investigated as a potential approach for treating liquid discharges. The FT-IR spectrum of the raw WNSp sample demonstrated that the WNSp waste was drastically modified following the adsorption process. SEM and XRD analyses revealed that the raw WNSp structure was less porous and more uniform as a result of MBD loading and the formation of a thick layer on the structure's surface after MBD adsorption. The obtained findings confirmed the BM dye's adsorption effectiveness onto raw WNSp. According to the thermodynamic parameters, the adsorption appeared to be exothermic and spontaneous. The spontaneous nature and feasibility of the MBD adsorption process on raw WNSp was proven by the negative standard enthalpy values (G°). The adsorption process kinetics were adequately defined by the pseudo-second-order model as the determination coefficient was equal to $R^2 = 0.999$ and an adsorbed amount of MBD per unit mass of the adsorbent material WNSp at equilibrium (q_e) was equal to 2.288 mg/g.

The findings of this study will contribute substantially to developing the use of raw walnut shell powder as a sustainable and green alternative for the removal of dyes from an aqueous solution.

Author Contributions: Conceptualization, S.F., M.M.Y., S.T. and S.L.; methodology, S.F.; software, S.F. and S.L.; validation and supervision, S.L. investigation, S.F.; writing—original draft preparation, S.F.; writing—review and editing, S.L. and M.M.Y.; visualization, H.T., M.K., M.Z., A.A., J.Z., A.H. and L.M.; project administration, S.L. All authors have read and agreed to the published version of the manuscript.

Funding: This research received no external funding.

Data Availability Statement: The data presented in this study are available in the manuscript.

Conflicts of Interest: The authors declare no conflict of interest.

References

1. Tahraoui, H.; Amrane, A.; Belhadj, A.-E.; Zhang, J. Modeling the Organic Matter of Water Using the Decision Tree Coupled with Bootstrap Aggregated and Least-Squares Boosting. *Environ. Technol. Innov.* **2022**, *27*, 102419. [CrossRef]
2. Tahraoui, H.; Belhadj, A.-E.; Hamitouche, A.; Bouhedda, M.; Amrane, A. Predicting the Concentration of Sulfate (SO42-) in Drinking Water Using Artificial Neural Networks: A Case Study: Médéa-Algeria. *Desalination Water Treat.* **2021**, *217*, 181–194. [CrossRef]
3. Tahraoui, H.; Belhadj, A.E.; Hamitouche, A.E. Prediction of the Bicarbonate Amount in Drinking Water in the Region of Médéa Using Artificial Neural Network Modelling. *Kem. Ind.* **2020**, *69*, 595–602. [CrossRef]
4. Habila, M.A.; ALOthman, Z.A.; Al-Tamrah, S.A.; Ghafar, A.A.; Soylak, M. Activated Carbon from Waste as an Efficient Adsorbent for Malathion for Detection and Removal Purposes. *J. Ind. Eng. Chem.* **2015**, *32*, 336–344. [CrossRef]
5. Alomar, T.S.; Habila, M.A.; AlMasoud, N.; Alothman, Z.A.; Sheikh, M.; Soylak, M. Biomass-Derived Adsorbent for Dispersive Solid-Phase Extraction of Cr (III), Fe (III), Co (II) and Ni (II) from Food Samples Prior to ICP-MS Detection. *Appl. Sci.* **2021**, *11*, 7792. [CrossRef]
6. Tahraoui, H.; Belhadj, A.-E.; Amrane, A.; Houssein, E.H. Predicting the Concentration of Sulfate Using Machine Learning Methods. *Earth Sci. Inform.* **2022**, *15*, 1023–1044. [CrossRef]
7. Alothman, Z.A.; Habila, M.A.; Moshab, M.S.; Al-Qahtani, K.M.; AlMasoud, N.; Al-Senani, G.M.; Al-Kadhi, N.S. Fabrication of Renewable Palm-Pruning Leaves Based Nano-Composite for Remediation of Heavy Metals Pollution. *Arab. J. Chem.* **2020**, *13*, 4936–4944. [CrossRef]
8. AlOthman, Z.A.; Habila, M.A.; Ali, R.; Ghafar, A.A.; Hassouna, M.S.E. Valorization of Two Waste Streams into Activated Carbon and Studying Its Adsorption Kinetics, Equilibrium Isotherms and Thermodynamics for Methylene Blue Removal. *Arab. J. Chem.* **2014**, *7*, 1148–1158. [CrossRef]
9. Dar, O.A.; Malik, M.A.; Talukdar, M.I.A.; Hashmi, A.A. Bionanocomposites in Water Treatment. In *Bionanocomposites*; Elsevier: Amsterdam, The Netherlands, 2020; pp. 505–518.
10. Thabede, P.M.; Shooto, N.D.; Naidoo, E.B. Removal of Methylene Blue Dye and Lead Ions from Aqueous Solution Using Activated Carbon from Black Cumin Seeds. *S. Afr. J. Chem. Eng.* **2020**, *33*, 39–50. [CrossRef]
11. Fu, Y.; Viraraghavan, T. Fungal Decolorization of Dye Wastewaters: A Review. *Bioresour. Technol.* **2001**, *79*, 251–262. [CrossRef]

12. Ginimuge, P.R.; Jyothi, S. Methylene Blue: Revisited. *J. Anaesthesiol. Clin. Pharmacol.* **2010**, *26*, 517–520. [CrossRef] [PubMed]
13. Sandoval, A.; Hernandez-Ventura, C.; Klimova, T.E. Titanate Nanotubes for Removal of Methylene Blue Dye by Combined Adsorption and Photocatalysis. *Fuel* **2017**, *198*, 22–30. [CrossRef]
14. Zahrim, A.Y.; Hilal, N. Treatment of Highly Concentrated Dye Solution by Coagulation/Flocculation–Sand Filtration and Nanofiltration. *Water Resour. Ind.* **2013**, *3*, 23–34. [CrossRef]
15. Houas, A.; Lachheb, H.; Ksibi, M.; Elaloui, E.; Guillard, C.; Herrmann, J.M. Photochemical Characterization and Photocatalytic Properties of a Nanostructure Composite TiO2 Film. *Appl. Catal. B Environ.* **2001**, *31*, 145–157. [CrossRef]
16. Ghuge, S.P.; Saroha, A.K. Catalytic Ozonation for the Treatment of Synthetic and Industrial Effluents-Application of Mesoporous Materials: A Review. *J. Environ. Manag.* **2018**, *211*, 83–102. [CrossRef]
17. Hadadi, A.; Imessaoudene, A.; Bollinger, J.-C.; Cheikh, S.; Assadi, A.A.; Amrane, A.; Kebir, M.; Mouni, L. Parametrical Study for the Effective Removal of Mordant Black 11 from Synthetic Solutions: Moringa Oleifera Seeds' Extracts Versus Alum. *Water* **2022**, *14*, 4109. [CrossRef]
18. Tahraoui, H.; Belhadj, A.-E.; Triki, Z.; Boudella, N.R.; Seder, S.; Amrane, A.; Zhang, J.; Moula, N.; Tifoura, A.; Ferhat, R.; et al. Mixed Coagulant-Flocculant Optimization for Pharmaceutical Effluent Pretreatment Using Response Surface Methodology and Gaussian Process Regression. *Process Saf. Environ. Prot.* **2023**, *169*, 909–927. [CrossRef]
19. Tahraoui, H.; Belhadj, A.E.; Moula, N.; Bouranene, S.; Amrane, A. Optimisation and Prediction of the Coagulant Dose for the Elimination of Organic Micropollutants Based on Turbidity. *Kem. Ind.* **2021**, *70*, 675–691. [CrossRef]
20. Allaoui, M.; Berradi, M.; Elharfi, A. Synthesis of a New Asymmetric Semi Permeable Membrane and Based Alloy of Two Polymers PVC and PSU. Application in the Treatment of a Colored Solution. *Moroc. J. Chem.* **2016**, *4*, 251–258.
21. Nasar, A.; Mashkoor, F. Application of Polyaniline-Based Adsorbents for Dye Removal from Water and Wastewater—A Review. *Environ. Sci. Pollut. Res.* **2019**, *26*, 5333–5356. [CrossRef]
22. Uddin, M.K. A Review on the Adsorption of Heavy Metals by Clay Minerals, with Special Focus on the Past Decade. *Chem. Eng. J.* **2017**, *308*, 438–462. [CrossRef]
23. Shakoor, S.; Nasar, A. Adsorptive Treatment of Hazardous Methylene Blue Dye from Artificially Contaminated Water Using Cucumis Sativus Peel Waste as a Low-Cost Adsorbent. *Groundw. Sustain. Dev.* **2017**, *5*, 152–159. [CrossRef]
24. Bouchelkia, N.; Mouni, L.; Belkhiri, L.; Bouzaza, A.; Bollinger, J.-C.; Madani, K.; Dahmoune, F. Removal of Lead (II) from Water Using Activated Carbon Developed from Jujube Stones, a Low-Cost Sorbent. *Sep. Sci. Technol.* **2016**, *51*, 1645–1653. [CrossRef]
25. Chudhary, Z.; Khera, R.A.; Hanif, M.A.; Ayub, M.A.; Hamrouni, L. Walnut. In *Medicinal Plants of South Asia*; Elsevier: Amsterdam, The Netherlands, 2020; pp. 671–684.
26. Liu, M.; Li, X.; Du, Y.; Han, R. Adsorption of Methyl Blue from Solution Using Walnut Shell and Reuse in a Secondary Adsorption for Congo Red. *Bioresour. Technol. Rep.* **2019**, *5*, 238–242. [CrossRef]
27. Wen, X.; Liu, H.; Zhang, L.; Zhang, J.; Fu, C.; Shi, X.; Chen, X.; Mijowska, E.; Chen, M.-J.; Wang, D.-Y. Large-Scale Converting Waste Coffee Grounds into Functional Carbon Materials as High-Efficient Adsorbent for Organic Dyes. *Bioresour. Technol.* **2019**, *272*, 92–98. [CrossRef]
28. Wong, S.; Tumari, H.H.; Ngadi, N.; Mohamed, N.B.; Hassan, O.; Mat, R.; Amin, N.A.S. Adsorption of Anionic Dyes on Spent Tea Leaves Modified with Polyethyleneimine (PEI-STL). *J. Clean. Prod.* **2019**, *206*, 394–406. [CrossRef]
29. Yu, Q.; Li, M.; Ji, X.; Qiu, Y.; Zhu, Y.; Leng, C. Characterization and Methanol Adsorption of Walnut-Shell Activated Carbon Prepared by KOH Activation. *J. Wuhan Univ. Technol.-Mater. Sci. Ed.* **2016**, *31*, 260–268. [CrossRef]
30. Albatrni, H.; Qiblawey, H.; Al-Marri, M.J. Walnut Shell Based Adsorbents: A Review Study on Preparation, Mechanism, and Application. *J. Water Process Eng.* **2022**, *45*, 102527. [CrossRef]
31. Ahmed, M.J.; Dhedan, S.K. Equilibrium Isotherms and Kinetics Modeling of Methylene Blue Adsorption on Agricultural Wastes-Based Activated Carbons. *Fluid Phase Equilibria* **2012**, *317*, 9–14. [CrossRef]
32. Kifuani, K.M.; Mayeko, A.K.K.; Vesituluta, P.N.; Lopaka, B.I.; Bakambo, G.E.; Mavinga, B.M.; Lunguya, J.M. Adsorption of Basic Dye, Methylene Blue, in Aqueous Solution on Bioadsorbent from Agricultural Waste of Cucumeropsis Mannii Naudin. *Int. J. Biol. Chem. Sci.* **2018**, *12*, 558–575. [CrossRef]
33. Miyah, Y.; Lahrichi, A.; Idrissi, M.; Boujraf, S.; Taouda, H.; Zerrouq, F. Assessment of Adsorption Kinetics for Removal Potential of Crystal Violet Dye from Aqueous Solutions Using Moroccan Pyrophyllite. *J. Assoc. Arab. Univ. Basic Appl. Sci.* **2017**, *23*, 20–28. [CrossRef]
34. Değermenci, G.D.; Değermenci, N.; Ayvaoğlu, V.; Durmaz, E.; Çakır, D.; Akan, E. Adsorption of Reactive Dyes on Lignocellulosic Waste; Characterization, Equilibrium, Kinetic and Thermodynamic Studies. *J. Clean. Prod.* **2019**, *225*, 1220–1229. [CrossRef]
35. Kuang, Y.; Zhang, X.; Zhou, S. Adsorption of Methylene Blue in Water onto Activated Carbon by Surfactant Modification. *Water* **2020**, *12*, 587. [CrossRef]
36. Uddin, M.; Rahman, M.; Rukanuzzaman, M.; Islam, M. A Potential Low Cost Adsorbent for the Removal of Cationic Dyes from Aqueous Solutions. *Appl. Water Sci.* **2017**, *7*, 2831–2842. [CrossRef]
37. de Yamil, L.O.; Georgin, J.; Franco, D.S.; Netto, M.S.; Grassi, P.; Piccilli, D.G.; Oliveira, M.L.; Dotto, G.L. Powdered Biosorbent from Pecan Pericarp (Carya Illinoensis) as an Efficient Material to Uptake Methyl Violet 2B from Effluents in Batch and Column Operations. *Adv. Powder Technol.* **2020**, *31*, 2843–2852.

38. Chan, S.-L.; Tan, Y.P.; Abdullah, A.H.; Ong, S.-T. Equilibrium, Kinetic and Thermodynamic Studies of a New Potential Biosorbent for the Removal of Basic Blue 3 and Congo Red Dyes: Pineapple (Ananas Comosus) Plant Stem. *J. Taiwan Inst. Chem. Eng.* **2016**, *61*, 306–315. [CrossRef]
39. Mashkoor, F.; Nasar, A.; Asiri, A.M. Exploring the Reusability of Synthetically Contaminated Wastewater Containing Crystal Violet Dye Using Tectona Grandis Sawdust as a Very Low-Cost Adsorbent. *Sci. Rep.* **2018**, *8*, 8314. [CrossRef]
40. Dahri, M.K.; Kooh, M.R.R.; Lim, L.B. Water Remediation Using Low Cost Adsorbent Walnut Shell for Removal of Malachite Green: Equilibrium, Kinetics, Thermodynamic and Regeneration Studies. *J. Environ. Chem. Eng.* **2014**, *2*, 1434–1444. [CrossRef]
41. Çelekli, A.; Birecikligil, S.S.; Geyik, F.; Bozkurt, H. Prediction of Removal Efficiency of Lanaset Red G on Walnut Husk Using Artificial Neural Network Model. *Bioresour. Technol.* **2012**, *103*, 64–70. [CrossRef]
42. Yang, J.; Qiu, K. Preparation of Activated Carbons from Walnut Shells via Vacuum Chemical Activation and Their Application for Methylene Blue Removal. *Chem. Eng. J.* **2010**, *165*, 209–217. [CrossRef]
43. Uddin, M.K.; Nasar, A. Walnut Shell Powder as a Low-Cost Adsorbent for Methylene Blue Dye: Isotherm, Kinetics, Thermodynamic, Desorption and Response Surface Methodology Examinations. *Sci. Rep.* **2020**, *10*, 7983. [CrossRef]
44. Almasi, A.; Rostamkhani, Z.; Mousavi, S.A. Adsorption of Reactive Red 2 Using Activated Carbon Prepared from Walnut Shell: Batch and Fixed Bed Studies. *Desalination Water Treat.* **2017**, *79*, 356–367. [CrossRef]
45. Almasi, A.; Navazeshkhaa, F.; Mousavi, S.A. Biosorption of Lead from Aqueous Solution onto Nasturtium Officinale: Performance and Modeling. *Desalination Water Treat.* **2017**, *65*, 443–450. [CrossRef]
46. Reçber, Z. Adsorption of Methylene Blue onto Spent Alchemilla Vulgaris Leaves: Characterization, Isotherms, Kinetic and Thermodynamic Studies. *Int. J. Environ. Sci. Technol.* **2022**, *19*, 4803–4814. [CrossRef]
47. Gad, H.M.H.; Omar, H.A.; Khalil, M.H.; Hassan, M.R. Factors Affecting Sorption of Pb (II) from Aqueous Solution Using Sawdust Based Activated Carbon. *J. Am. Sci.* **2013**, *9*, 95–106.
48. Miyah, Y.; Lahrichi, A.; Idrissi, M.; Khalil, A.; Zerrouq, F. Adsorption of Methylene Blue Dye from Aqueous Solutions onto Walnut Shells Powder: Equilibrium and Kinetic Studies. *Surf. Interfaces* **2018**, *11*, 74–81. [CrossRef]
49. Khelifi, O.; Mehrez, I. Equilibrium, Kinetics and Thermodynamics Studies of Methylene Blue Adsorption from Aqueous Solutions by Biosorbent Derived from Algerian Date Stones. *J. Water Sci. Environ. Technol.* **2016**, *2*, 32–38.
50. Lansari, F.; Edjekouane, M.; Khelifi, O.; Boukheteche, I.; Laksaci, H. Elimination of Methylene Blue by Low-Cost Biomaterial Prepared from Local Natural Residue. *Alger. J. Renew. Energy Sustain. Dev.* **2020**, *2*, 60–66. [CrossRef]
51. Zeghoud, L.; Gouamid, M.; Ben Mya, O.; Rebiai, A.; Saidi, M. Adsorption of Methylene Blue Dye from Aqueous Solutions Using Two Different Parts of Palm Tree: Palm Frond Base and Palm Leaflets. *Water AirSoil Pollut.* **2019**, *230*, 195. [CrossRef]
52. Dbik, A.; El Messaoudi, N.; Bentahar, S.; El Khomri, M.; Lacherai, A.; Faska, N. Optimization of Methylene Blue Adsorption on Agricultural Solid Waste Using Box–Behnken Design (BBD) Combined with Response Surface Methodology (RSM) Modeling. *Biointerface Res. Appl. Chem.* **2022**, *12*, 4567–4583.
53. Nuhoğlu, Y.; Ekmekyapar Kul, Z.; Kul, S.; Nuhoğlu, Ç.; Ekmekyapar Torun, F. Pb (II) Biosorption from the Aqueous Solutions by Raw and Modified Tea Factory Waste (TFW). *Int. J. Environ. Sci. Technol.* **2021**, *18*, 2975–2986. [CrossRef]
54. Nordine, N.; El Bahri, Z.; Sehil, H.; Fertout, R.I.; Rais, Z.; Bengharez, Z. Lead Removal Kinetics from Synthetic Effluents Using Algerian Pine, Beech and Fir Sawdust's: Optimization and Adsorption Mechanism. *Appl. Water Sci.* **2016**, *6*, 349–358. [CrossRef]
55. Langmuir, I. The Constitution and Fundamental Properties of Solids and Liquids. Part I. Solids. *J. Am. Chem. Soc.* **1916**, *38*, 2221–2295. [CrossRef]
56. Freundlich, H. Über Die Adsorption in Lösungen. *Z. Phys. Chem.* **1907**, *57*, 385–470. [CrossRef]
57. Giles, C.H.; MacEwan, T.H.; Nakhwa, S.N.; Smith, D. A System of Classification of Solution Adsorption Isotherms, and Its Use in Diagnosis of Adsorption Mechanisms and in Measurement of Specific Surface Areas of Solids. *J. Chem. Soc.* **1960**, *111*, 3973–3993. [CrossRef]
58. Mousavi, S.A.; Mahmoudi, A.; Amiri, S.; Darvishi, P.; Noori, E. Methylene Blue Removal Using Grape Leaves Waste: Optimization and Modeling. *Appl. Water Sci.* **2022**, *12*, 112. [CrossRef]
59. Kocaman, S. Removal of Methylene Blue Dye from Aqueous Solutions by Adsorption on Levulinic Acid-Modified Natural Shells. *Int. J. Phytoremediation* **2020**, *22*, 885–895. [CrossRef]
60. Eltaweil, A.S.; Elgarhy, G.S.; El-Subruiti, G.M.; Omer, A.M. Carboxymethyl Cellulose/Carboxylated Graphene Oxide Composite Microbeads for Efficient Adsorption of Cationic Methylene Blue Dye. *Int. J. Biol. Macromol.* **2020**, *154*, 307–318. [CrossRef]
61. Jawad, A.H.; Abdulhameed, A.S.; Wilson, L.D.; Syed-Hassan, S.S.A.; ALOthman, Z.A.; Khan, M.R. High Surface Area and Mesoporous Activated Carbon from KOH-Activated Dragon Fruit Peels for Methylene Blue Dye Adsorption: Optimization and Mechanism Study. *Chin. J. Chem. Eng.* **2021**, *32*, 281–290. [CrossRef]
62. Jawad, A.H.; Abdulhameed, A.S.; Mastuli, M.S. Acid-Factionalized Biomass Material for Methylene Blue Dye Removal: A Comprehensive Adsorption and Mechanism Study. *J. Taibah Univ. Sci.* **2020**, *14*, 305–313. [CrossRef]
63. Sah, M.K.; Edbey, K.; EL-Hashani, A.; Almshety, S.; Mauro, L.; Alomar, T.S.; AlMasoud, N.; Bhattarai, A. Exploring the Biosorption of Methylene Blue Dye onto Agricultural Products: A Critical Review. *Separations* **2022**, *9*, 256. [CrossRef]
64. Ramutshatsha-Makhwedzha, D.; Mavhungu, A.; Moropeng, M.L.; Mbaya, R. Activated Carbon Derived from Waste Orange and Lemon Peels for the Adsorption of Methyl Orange and Methylene Blue Dyes from Wastewater. *Heliyon* **2022**, *8*, e09930. [CrossRef] [PubMed]

65. Reddy, M.S.; Sivaramakrishna, L.; Reddy, A.V. The Use of an Agricultural Waste Material, Jujuba Seeds for the Removal of Anionic Dye (Congo Red) from Aqueous Medium. *J. Hazard. Mater.* **2012**, *203*, 118–127. [CrossRef]
66. Benhachem, F.Z.; Attar, T.; Bouabdallah, F. Kinetic Study of Adsorption Methylene Blue Dye from Aqueous Solutions Using Activated Carbon. *Chem. Rev. Lett.* **2019**, *2*, 33–39.
67. Chakraborty, T.W.; Weber, R.K. Pore and Solid Diffusion Model for Fixed Bed Adsorbents. *J. Am. Inst. Chem. Eng.* **1974**, *20*, 228.
68. Ooi, J.; Lee, L.Y.; Hiew, B.Y.Z.; Thangalazhy-Gopakumar, S.; Lim, S.S.; Gan, S. Assessment of Fish Scales Waste as a Low Cost and Eco-Friendly Adsorbent for Removal of an Azo Dye: Equilibrium, Kinetic and Thermodynamic Studies. *Bioresour. Technol.* **2017**, *245*, 656–664. [CrossRef]
69. Anastopoulos, I.; Margiotoudis, I.; Massas, I. The Use of Olive Tree Pruning Waste Compost to Sequestrate Methylene Blue Dye from Aqueous Solution. *Int. J. Phytoremediat.* **2018**, *20*, 831–838. [CrossRef]
70. Lagergren, S.K. About the Theory of So-Called Adsorption of Soluble Substances. *Sven. Vetenskapsakad. Handingarl* **1898**, *24*, 1–39. Available online: https://cir.nii.ac.jp/all?q=Sven.%20Vetenskapsakad.%20Handingarl (accessed on 31 December 2022).
71. Ho, Y.S.; Ng, J.C.; McKay, G. Sorption of dye from aqueous solution by peat. *Chem. Eng. J.* **1998**, *70*, 115–124. [CrossRef]
72. Zamouche, M.; Mouni, L.; Ayachi, A.; Merniz, I. Use of Commercial Activated Carbon for the Purification of Synthetic Water Polluted by a Pharmaceutical Product. *Desalination Water Treat.* **2019**, *172*, 86–95. [CrossRef]
73. Sulthana, R.; Taqui, S.N.; Zameer, F.; Syed, U.T.; Syed, A.A. Adsorption of Ethidium Bromide from Aqueous Solution onto Nutraceutical Industrial Fennel Seed Spent: Kinetics and Thermodynamics Modeling Studies. *Int. J. Phytoremediation* **2018**, *20*, 1075–1086. [CrossRef] [PubMed]
74. Munagapati, V.S.; Wen, J.-C.; Pan, C.-L.; Gutha, Y.; Wen, J.-H.; Reddy, G.M. Adsorptive Removal of Anionic Dye (Reactive Black 5) from Aqueous Solution Using Chemically Modified Banana Peel Powder: Kinetic, Isotherm, Thermodynamic, and Reusability Studies. *Int. J. Phytoremediat.* **2020**, *22*, 267–278. [CrossRef] [PubMed]
75. Zhang, Y.; Wang, W.; Zhang, J.; Liu, P.; Wang, A. A Comparative Study about Adsorption of Natural Palygorskite for Methylene Blue. *Chem. Eng. J.* **2015**, *262*, 390–398. [CrossRef]
76. Ammendola, P.; Raganati, F.; Chirone, R. CO2 Adsorption on a Fine Activated Carbon in a Sound Assisted Fluidized Bed: Thermodynamics and Kinetics. *Chem. Eng. J.* **2017**, *322*, 302–313. [CrossRef]
77. Bouhedda, M.; Lefnaoui, S.; Rebouh, S.; Yahoum, M.M. Predictive Model Based on Adaptive Neuro-Fuzzy Inference System for Estimation of Cephalexin Adsorption on the Octenyl Succinic Anhydride Starch. *Chemom. Intell. Lab. Syst.* **2019**, *193*, 103843. [CrossRef]
78. Souidi, R.; Belarbi, L.; Bousalem, S. Methylene Blue Adsorption from Aqueous Solution by Low Cost Vine-Wood Biomass. 2021. Available online: https://assets.researchsquare.com/files/rs-141359/v1_covered.pdf?c=1631851536 (accessed on 31 December 2022).
79. Bouchelkia, N.; Tahraoui, H.; Amrane, A.; Belkacemi, H.; Bollinger, J.-C.; Bouzaza, A.; Zoukel, A.; Zhang, J.; Mouni, L. Jujube Stones Based Highly Efficient Activated Carbon for Methylene Blue Adsorption: Kinetics and Isotherms Modeling, Thermodynamics and Mechanism Study, Optimization via Response Surface Methodology and Machine Learning Approaches. *Process Saf. Environ. Prot.* **2022**, *170*, 513–535. [CrossRef]